THE JOURNAL OF BIOLOGICAL CHEMISTRY
Vol. 276, No. 23, Issue of June 8, pp. 20566–20571, 2001

Printed in U.S.A.

Directed Inhibition of Nuclear Import in Cellular Hypertrophy*

Received for publication, March 5, 2001
Published, JBC Papers in Press, March 30, 2001, DOI 10.1074/jbc.M101950200

Carmen Perez-Terzic‡§¶, A. Marquis Gacy§, Ryan Bortolon§, Petras P. Dzeja‡§, Michel Puceat‡‖, Marisa Jaconi‡, Franklyn G. Prendergast§, and Andre Terzic‡§‡‡**

From the ‡Division of Cardiovascular Diseases, Department of Medicine, the §Department of Molecular Pharmacology and Experimental Therapeutics, and the ¶Department of Physical Medicine and Rehabilitation, Mayo Clinic, Mayo Foundation, Rochester, Minnesota 55905

Each nuclear pore is responsible for both nuclear import and export with a finite capacity for bidirectional transport across the nuclear envelope. It remains poorly understood how the nuclear transport pathway responds to increased demands for nucleocytoplasmic communication. A case in point is cellular hypertrophy in which increased amounts of genetic material need to be transported from the nucleus to the cytosol. Here, we report an adaptive down-regulation of nuclear import supporting such an increased demand for nuclear export. The induction of cardiac cell hypertrophy by phenylephrine or angiotensin II inhibited the nuclear translocation of H1 histones. The removal of hypertrophic stimuli reversed the hypertrophic phenotype and restored nuclear import. Moreover, the inhibition of nuclear export by leptomycin B rescued import. Hypertrophic reprogramming increased the intracellular GTP/GDP ratio and promoted the nuclear redistribution of the GTP-binding transport factor Ran, favoring export over import. Further, in hypertrophy, the reduced creatine kinase and adenylate kinase activities limited energy delivery to the nuclear pore. The reduction of activities was associated with the closure of the cytoplasmic phase of the nuclear pore preventing import at the translocation step. Thus, to overcome the limited capacity for nucleocytoplasmic transport, cells requiring increased nuclear export regulate the nuclear transport pathway by undergoing a metabolic and structural restriction of nuclear import.

Hypertrophy is a fundamental adaptive process that enables heart muscle to accommodate demands for increased workload or to compensate for the loss of cardiac cells (1–3). Hypertrophied cardiomyocytes display a distinct pattern of gene expression, increased content of contractile proteins, and augmented myofibrillogenesis (1–8). Such critical processes in hypertrophy depend on molecules that have to be carried into or out of the nucleus (9, 10). In particular, the amount of mRNAs that need to be transported from the nucleus to the cytosol and transcribed into proteins dramatically increases (1–3, 11–13). Considering the limited total capacity for nuclear transport (14–17), it remains unknown how the nuclear transport pathway operates to support increased demands for nucleocytoplasmic communication.

The nuclear envelope, which separates the nuclear content from the cytoplasm, mediates the transport required for the regulation of gene expression and processing of genetic information (14–16). Although several steps in the process are recognized including targeting and movement to the nuclear surface, it is translocation through the nuclear envelope that ultimately secures the transfer of molecules (17–23). Translocation occurs through nuclear pore complexes, which span the nuclear envelope and gate bidirectional nucleocytoplasmic exchange (24–26). In response to changes in cellular bioenergetics or ion homeostasis, nuclear pores adopt distinct conformations regulating nuclear import (24–29). Transport can be activated and inactivated during the cell cycle (30), indicating that traffic through the nuclear pores is a dynamic process determined by the functional and metabolic state of a cell.

We report a down-regulated nuclear import in hypertrophy, which is restored by the removal of the hypertrophic signal or blockade of nuclear export. Thus, cardiac cells suppress nuclear import under conditions of increased demand for nucleocytoplasmic communication to secure the availability of the nuclear transport pathways required for the generation of the hypertrophic phenotype.

EXPERIMENTAL PROCEDURES

Hypertrophy—Hearts were removed from 1–2-day-old rats, and cardiomyocytes were isolated and cultured (29). Hypertrophy was induced with phenylephrine (100 μM), an α-adrenoreceptor agonist (in the presence of 10 μM propranolol, a β-adrenoreceptor antagonist), or with angiotensin II (100 nM). Myocyte size and sarcomeric α-actin content were used as markers of hypertrophy (4). Size was quantified by measuring the cell surface area with laser confocal microscopy (LSM 410 Carl Zeiss) and a × 40 (1.3 NA) objective. The expression of α-actin was determined by phalloidin staining that recognizes sarcomeric actin. To this end, cells fixed with 3% paraformaldehyde were incubated (20 min) with 20 nM phalloidin tagged with fluorescein, washed in 3% Tween in phosphate-buffered saline, and imaged by laser confocal microscopy using a × 63 (1.4 NA) objective. The light source was an argon/krypton laser tuned at 488 nm, and emission light was collected using a 510-nm-long pass dichroic beam splitter and a 515-nm-long pass emission filter. Two-dimensional confocal images were acquired by scanning 512 × 512 pixels per image and processed on a Silicon Graphics Iris Computer with ANALYZE software (Mayo Foundation).

Microinjections—Control or hypertrophied cardiomyocytes were transferred to prewarmed Dulbecco's modified Eagle's medium with 0.5% bovine serum albumin, 10 mM HEPES (pH 7.5), and 20 mM 2,3-butanedione monoxime (Sigma). Microinjections into the cytosol were carried out with a nanometer-precision microinjector unit (Eppendorf 5242) coupled to a micromanipulator (Eppendorf 5171) mounted on

* This work was supported by the American Heart Association, the Clinician-Investigator Program at the Mayo Clinic, the Miami Heart Research Institute, the Bruce and Ruth Rappaport Program in Vascular Biology and Gene Delivery, and the Marriott Foundation and by Grants HL64822 and HL07111 from the National Institutes of Health. The costs of publication of this article were defrayed in part by the payment of page charges. This article must therefore be hereby marked "*advertisement*" in accordance with 18 U.S.C. Section 1734 solely to indicate this fact.

‖ Present address: CNRS CRBM UPR1086, Montpellier, France.

** Present address: Department of Geriatrics, University of Geneva, Geneva, Switzerland.

‡‡ An Established Investigator of the American Heart Association. To whom correspondence should be addressed: Guggenheim 7, Mayo Clinic, Rochester, MN 55905. Tel.: 507-284-2747; Fax: 507-284-9111; E-mail: terzic.andre@mayo.edu.

a fluorescence microscope (Carl Zeiss Axiovert 100) (29, 31). Pipettes were filled with injection buffer (150 mM KCl, 1 mM PIPES,[1] 0.1 mM EDTA, 0.025 mM EGTA, pH 7.2) containing fluorescein-coupled histones H1 (0.07 mg/ml) or fluorescein-coupled dextrans (5 mM).

Nuclear Transport—Cardiomyocytes were superfused with 116 mM NaCl, 4 mM KCl, 2 mM $MgCl_2$, 2 mM NaH_2PO_4, 4 mM $NaHCO_3$, 21 mM HEPES, and 1 mM $CaCl_2$ (pH 7.4, 37 °C). Nuclear transport was measured using × 40 (1.3 NA) or × 63 (1.4 NA) objectives on a laser confocal imaging system (LSM 410). The thickness of the optical sections of imaged cells was set at 1–2 μm to discriminate fluorescence emitted from nuclear *versus* nonnuclear regions. Fluorescent probes were excited (at 488 nm) using an argon/krypton visible laser (Omnichrome), and emission spectra were collected using a 510-nm-long pass dichroic beam splitter and a 515-nm-long pass emission filter. Confocal images were acquired by scanning a field at 16 s/frame. Fluorescence intensity in the nucleus *versus* the cytosol was determined with ANALYZE on a Silicon Graphics Iris computer. Nuclear accumulation was expressed as the ratio of nuclear over cytosolic fluorescence (27, 29).

Ran Immunofluorescence—To localize the monomeric GTPase Ran, cardiomyocytes were fixed, permeabilized, and labeled with an anti-Ran monoclonal antibody (32). Optical z-sections of cells (0.2 μm) were acquired with a 1300 YHS CCD camera (Princeton Instruments) using an objective mounted on a piezoelectric controller driven by the Metamorph software (Universal Imaging) (33). Images were processed by the Imaris software (Bitplane) using the isosurface module (for three-dimensional reconstruction) following digital deconvolution (Huygens, Scientific Volume Imaging) (33).

Nucleotides—To determine nucleotide levels, perchloric acid cardiomyocyte extracts were prepared (34). Cells, washed with ice-cold phosphate-buffered saline and immersed into liquid nitrogen, were layered with 0.6 M $HClO_4$ and 1 mM EDTA and then centrifuged (12,000 rpm, 4 °C) (Hermline Z230 MA microcentrifuge, Labnet). The supernatant was neutralized with 2 M K_2HCO_3, and the precipitate was removed by centrifugation. ATP was measured in the supernatant by using a coupled enzyme assay in 25 mM Tris-HCl buffer (pH 7.5), 2 mM $MgCl_2$, 2 mM glucose, 1 mM dithiothreitol, 50 μM $NADP^+$, 20 μM diadenosine pentaphosphate, 4 units/ml of hexokinase, and 2 units/ml of glucose-6-phosphate dehydrogenase. NADPH levels, reflecting ATP concentration, were measured using a fluorometer with a minicell kit (Turner TD-700). ATP, GTP, and GDP were also determined by HPLC (System Gold, Beckman) using a QHR5/5 column (Amersham Pharmacia Biotech). Nucleotides were eluted with a linear gradient of triethylammonium bicarbonate buffer.

Enzyme Activities—Cells were extracted with 150 mM NaCl, 60 mM Tris-HCl (pH 7.5), 5 mM EDTA, 1 mM phenylmethylsulfonyl fluoride, 10 μg/ml leupeptin, 1 μg/ml aprotinin, and 0.2% Triton X-100 and were then centrifuged (10,000 × *g*, 4 °C). Creatine kinase activity was measured with a Beckman DU 7400 spectrophotometer in 100 mM Tris acetate (pH 7.5), 20 mM glucose, 2 mM EDTA, 10 mM $MgCl_2$, 2 mM dithiothreitol, 2 mM $NADP^+$, 2 mM ADP, 5 mM AMP, 20 mM creatine phosphate, 20 μM diadenosine pentaphosphate, 4.5 units/ml hexokinase, and 2 units/ml glucose-6-phosphate dehydrogenase (35). Adenylate kinase was measured in 100 mM potassium acetate, 20 mM HEPES (pH 7.5), 20 mM glucose, 4 mM $MgCl_2$, 2 mM $NADP^+$, 1 mM EDTA, 1 mM dithiothreitol, 2 mM ADP, 4.5 units/ml hexokinase, and 2 units/ml glucose-6-phosphate dehydrogenase (35).

Electron Microscopy—Cardiac nuclei were imaged with transmitted and field-emission scanning electron microscopy (FESEM). Cardiomyocytes were fixed in 0.1 M phosphate-buffered saline containing 1% glutaraldehyde and 4% formaldehyde (pH 7.2). For transmitted scanning electron microscopy, cells were postfixed in phosphate-buffered 1% OsO_4, stained *en bloc* with 2% uranyl acetate, dehydrated in ethanol and propylene oxide, and embedded in low viscosity epoxy resin. Thin (90-nm) sections were cut on an ultramicrotome (Reichert Ultracut E), placed on 200-μm mesh copper grids, and stained with lead citrate. Micrographs were taken on a JEOL 1200 EXII electron microscope operating at 60 kV. For FESEM, cardiomyocytes were stripped of sarcolemma by using a hypotonic solution followed by a 5-min treatment with 1% Triton X-100 (29). Sarcolemma-stripped cardiomyocytes were fixed *in situ* with 1% glutaraldehyde and 4% formaldehyde in phosphate-buffered saline (pH 7.2). The specimen was rinsed in 0.1 M phosphate buffer (pH 7.2), and the buffer was supplemented with 1% osmium. Cells, which were dehydrated with ethanol and dried in a critical point dryer, were coated with platinum using an Ion Tech indirect argon ion voltage of 9.5 kV and 4.2 mA and then examined at accelerating voltages (1.0, 2.4, 3.5, and 5.0 kV) on a JEOL JSM 6400 field-emission scanning microscope.

[1] The abbreviations used are: PIPES, 1,4-piperazinediethanesulfonic acid; HPLC, high pressure liquid chromatography; fl-H1, fluorescein-tagged histone 1; FESEM, field-emission scanning electron microscopy; AFM, atomic force microscopy.

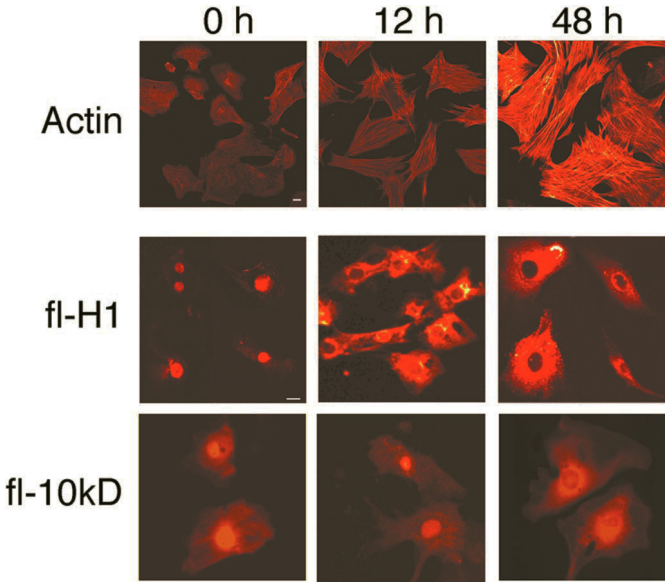

FIG. 1. **Down-regulated nuclear import in hypertrophy.** *Upper row*, laser confocal microscopy of neonatal cardiomyocytes at 0, 12, and 48 h following the addition of phenylephrine (100 μM), a hypertrophic stimulator. Actin was labeled with fluorescein-tagged phalloidin. *Middle and lower rows*, fl-H1 or 10-kDa dextrans (*fl-10 kDa*) were microinjected into the cytosol of control (0 h) or hypertrophied (12 or 48 h after the addition of 100 μM phenylephrine) cardiomyocytes. Although readily imported in control cardiomyocytes, H1 histones were excluded from the nucleus of hypertrophied cardiomyocytes (*middle row*). The passive nuclear diffusion of dextrans was maintained up to 48 h in hypertrophy (*lower row*). *Horizontal bars*, 10 μm. *Vertical bars*, fluorescence scale.

Atomic Force Microscopy—Contact-mode atomic force microscopy (AFM) was performed in air with silicon nitride NP-S tips (spring constant, 0.58 newtons/m) using a Digital Instruments Multimode AFM with a Nanoscope III controller (29). The nuclear envelope of sarcolemma-stripped and fixed cardiomyocytes was scanned with an E-type (15 × 15 μm maximum area) scanner. Images were collected by raster scanning at 512 pixels/line with linear scanning frequencies ranging from 5 to 15 Hz to build 512 × 512 pixel images. AFM images were analyzed using Nanoscope IIIa software, and three-dimensional images were generated from topographical height information. Open and closed states of individual nuclear pore complexes were determined from 3 × 3 μm scans.

Statistics—Results are expressed as mean ± S.E. Statistical analysis was carried out by the Student's *t* test. The significant difference was accepted at the $p < 0.05$ level.

RESULTS

Down-regulated Nuclear Import in Hypertrophy—Neonatal cardiomyocytes treated with growth factors such as α_1-adrenoreceptor agonists are an established cell system of hypertrophy (9, 12). Within 12 h of phenylephrine treatment (100 μM), cardiomyocytes nearly doubled in size from 655 ± 49 μm^2 (n = 40) to 1158 ± 91 μm^2 (n = 21) and markedly increased their content of actin filaments organized in contractile myofibrils (Fig. 1). Cardiomyocytes further enlarged to 1580 ± 143 μm^2 (n = 32) and 1950 ± 177 μm^2 (n = 28) at 24 and 48 h following phenylephrine treatment.

Histones, major constituents of eukaryotic chromatin, are imported into nuclei by active transport (36–38). When microinjected into the cytosol of control cardiomyocytes, fluorescein-tagged histone 1 (fl-H1) were readily transported into the nucleus, resulting in pronounced nuclear fluorescence (Fig. 1). However, early in hypertrophy, the active import of fl-H1 was

down-regulated with the nuclear/cytoplasmic ratio, an index of nuclear transport (27, 29, 39), decreasing by 74% from 3.18 ± 0.23 (n = 54) to 0.82 ± 0.12 (n = 7) within 12 h following the addition of phenylephrine ($p < 0.05$) (Fig. 1). With prolonged hypertrophy (48 h), the import of fl-H1 remained at reduced levels with the nuclear/cytoplasmic ratio of 0.74 ± 0.20 (n = 59) (Fig. 1).

To determine whether the down-regulated transport of fl-H1 was attributable to hypertrophy rather than to a nonhypertrophy-related effect of phenylephrine, we evaluated nuclear transport in cells in which hypertrophy was induced through another receptor system. Angiotensin II (100 nM), which acts via angiotensin receptors (12), also induced hypertrophy, and the cell surface increased from 933 ± 57 μm^2 (n = 81) to 2176 ± 288 μm^2 (n = 24 at 48 h of treatment). In angiotensin II-treated cells, the nuclear import of fl-H1 was also rapidly reduced within 12 h, and the nuclear/cytoplasmic ratio decreased by 57% (from 3.35 ± 0.23, n = 47 to 1.43 ± 0.34, n = 12; $p < 0.05$).

Like phenylephrine and angiotensin II, the purinergic agonist ATP activates the phosphoinositide pathway without, however, inducing hypertrophy (40). Inositol trisphosphate, a product of this pathway, releases Ca^{2+} from the nuclear cisterna and can inhibit nuclear import (27, 39, 41). To exclude the possibility that impaired transport in hypertrophied cells was attributable to the inositol trisphosphate-induced decrease in cisternal Ca^{2+}, we examined cells treated with ATP (50 μM, 48 h). ATP did not increase the cell size or actin content (40), but it activated phosphoinositide turnover (42). The cell surface was 582 ± 36 μm^2 (n = 81) and 618 ± 43 μm^2 (n = 62) in untreated and ATP-treated cells, respectively ($p > 0.05$). In ATP-treated cells, even following prolonged exposure (48 h) to the purinergic agonist, fl-H1 was readily imported in the nucleus. The nuclear/cytoplasmic ratio for fl-H1 was 3.35 ± 0.23 (n = 47) and 3.12 ± 0.33 (n = 6) in controls and ATP-treated cells ($p > 0.05$), respectively. Thus, the down-regulation of active nuclear import is concomitant with the development of cell hypertrophy.

Delayed Inhibition of Nuclear Passive Diffusion in Hypertrophy—Small molecular weight molecules such as dextrans commonly lack a nuclear localization signal and passively diffuse into the nucleus (39). When microinjected into the cytosol, fluorescein-conjugated 10-kDa dextrans diffused readily into the nucleus of control cells (Fig. 1). With the development of hypertrophy, passive diffusion appeared unaltered with nuclear/cytoplasmic ratios at 1.66 ± 0.12 (n = 12; 12 h) and 1.78 ± 0.08 (n = 17; 24 h), values not significantly different from the control ratio of 1.58 ± 0.18 (n = 4; $p > 0.05$) (Fig. 1). The passive diffusion of 10-kDa dextrans decreased only in the advanced stages of hypertrophy. In fact, 48 h was required after the initiation of hypertrophy for a significant reduction in the nucleocytoplasmic ratio (0.65 ± 0.04; n = 5) (Fig. 1). Even smaller molecules such as 3-kDa dextrans demonstrate unregulated diffusion across the nuclear membrane (27, 29) regardless of the hypertrophic state. The nuclear/cytoplasmic ratio for 3-kDa dextrans was 1.92 ± 0.10 (n = 16) in control and 1.99 ± 0.10 (n = 14) following 48 h of phenylephrine treatment ($p > 0.05$).

Removal of the Hypertrophic Signal Restores Nuclear Import—With the removal of the α_1-adrenoreceptor agonist, cells progressively returned to their original sizes. At 48 and 72 h after the withdrawal of phenylephrine, the cell surface was 910 ± 103 μm^2 (n = 11) and 750 ± 40 μm^2 (n = 77), respectively, values close to those obtained prior to hypertrophy (Fig. 2). With the reversal of the hypertrophic phenotype, active nuclear import was partially restored with a nuclear/cytoplasmic ratio of 1.94 ± 0.21 (n = 11). This represents an increase of

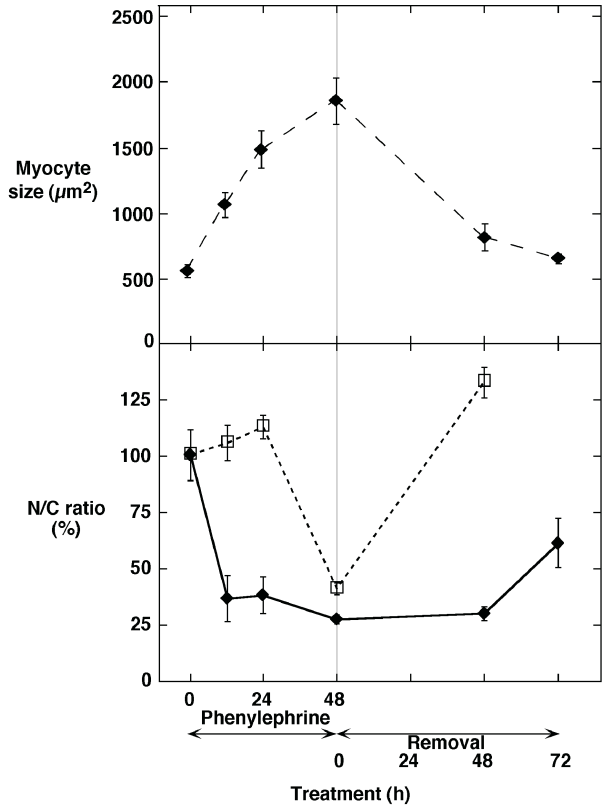

FIG. 2. **Time-course of inhibition and restoration of nuclear import.** *Upper panel*, cell enlargement in the presence of phenylephrine (100 μM) and the restoration of original cell size following the removal of the hypertrophic stimulus. Each *symbol* represents a mean value obtained from 40 to 77 cardiomyocytes. *Lower panel*, nuclear/cytoplasmic (N/C) ratio of histone H1 (*filled diamonds*, *continuous line*) and 10-kDa dextrans (*open squares*, *dotted line*) in the presence of phenylephrine or after its removal. Each *symbol* represents a mean value obtained from 4 to 17 cardiomyocytes.

61% of the control, compared with ~25% of the control at 12 and 48 h of hypertrophy (Fig. 2). With the removal of the hypertrophic stimulus, passive nuclear diffusion promptly returned to prehypertrophy values with a nuclear/cytoplasmic ratio of 2.08 ± 0.10 (n = 9) within 48 h of phenylephrine withdrawal (Fig. 2). Thus, the increase in cell size and the down-regulation of nuclear import are reversed on the removal of the hypertrophic signal.

Hypertrophy Favors Export through Redistribution of Nuclear Transport Factors—With hypertrophy, a more dense actin network may have impeded transfer to the nuclear surface, thereby precluding nuclear import. Cytochalasin B (20 μM), a disrupter of the cytoskeleton (43), reduced the organized actin networks but did not improve nuclear import in hypertrophied cells (data not shown). Rather, in hypertrophy an increased amount of mRNA needs to be transported from the nucleus into the cytosol (1–3, 9, 11). Optimal nuclear export requires a high cellular GTP/GDP ratio along with the nuclear availability of the GTP-binding protein Ran (20, 21, 32). Here, the GTP/GDP ratio increased from 2.7 in normal cardiomyocytes to 3.6 in hypertrophied cardiomyocytes (Fig. 3*a*). Moreover, Ran immunofluorescence, although diffusely distributed throughout the control cardiomyocytes, was primarily confined to the nucleus of hypertrophied cells (Fig. 3, *a–c*). Thus, cellular hypertrophy promotes the rearrangement of nuclear transport factors that favor export over import.

Inhibition of Nuclear Export Restores Import—The *Streptomyces* metabolite leptomycin B is a potent inhibitor of nuclear export through binding to exportin, the export shuttle protein

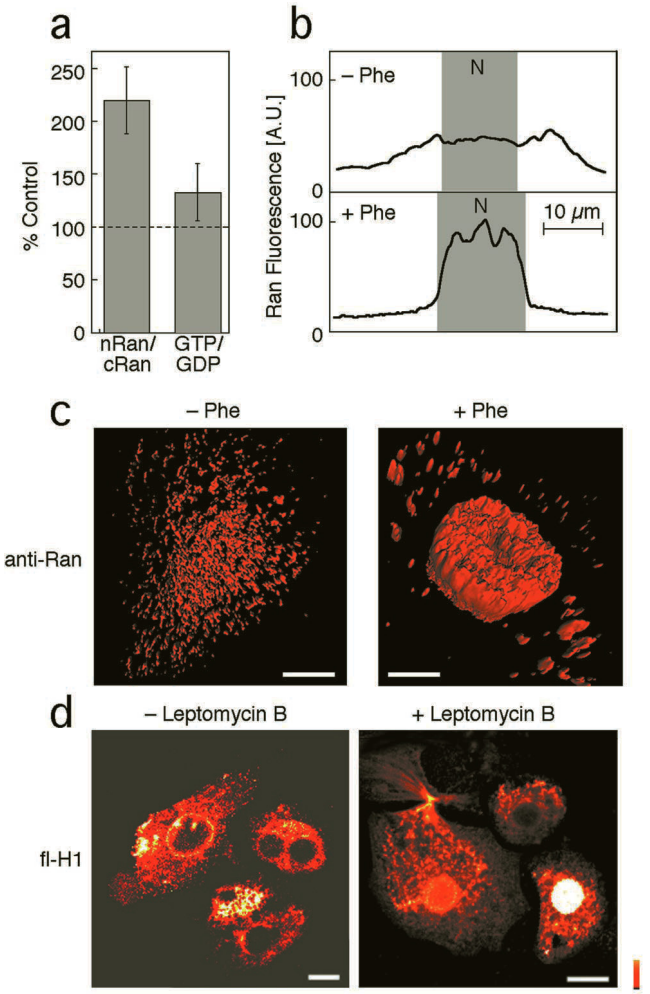

FIG. 3. **Nuclear export favored over import in hypertrophy.** *a*, increased GTP/GDP ratio and nuclear trapping of Ran in hypertrophied cardiomyocytes. Values are expressed as percent over control. *nRan*, nuclear Ran; *cRan*, cytosolic Ran. *b*, a topographic section of Ran immunofluorescence in control (*−Phe*) and hypertrophied (*+Phe*) cardiomyocytes shows the dramatic nuclear accumulation of Ran in hypertrophy. *N*, nuclear region; *bar*, 10 μm. *c*, three-dimensional reconstruction of the nucleus and surrounding region labeled with an anti-Ran antibody demonstrating a diffuse *versus* nuclear-limited pattern of Ran distribution in control (*−Phe*) and hypertrophied (*+Phe*) cells, respectively. *Bar*, 5 μm. *d*, the nuclear export inhibitor leptomycin B restores nuclear import in hypertrophied cells. H1 was microinjected into the cytosol of hypertrophied cardiomyocytes untreated (*left*) or treated (*right*) with the nuclear export inhibitor leptomycin B (10 nM, 4 h). Hypertrophy was induced by phenylephrine (100 μM, 48 h). The laser scanning confocal images indicate the exclusion of H1 from the nucleus of hypertrophied cardiomyocytes without, and partial restoration of nuclear import with, leptomycin. *Horizontal bars*, 15 μm; *vertical bar*, relative fluorescence scale.

(44). The treatment of hypertrophied cardiomyocytes with 10 nM leptomycin B, a concentration that blocks nuclear export (44–46), restored the nuclear import of fl-H1 in the majority of cells (Fig. 3*d*). The nuclear import of fl-H1 in hypertrophied cells was 0.29 ± 0.08 ($n = 9$) but increased 7-fold to 2.23 ± 0.50 ($n = 11$; $p < 0.05$) after leptomycin treatment. Thus, down-regulated nuclear import in hypertrophy can be rescued by an inhibitor of nuclear export.

Reduced Nucleotide Levels and Phosphotransfer Activities in Hypertrophy Further Impede Nuclear Import—ATP and GTP provide energy for nuclear transport or regulate the assembly and disassembly of transport complexes (15, 16, 47). The depletion of energy stores inhibits nuclear import (29). Here, in hypertrophied cells, ATP was reduced from 23 ± 2 to 19 ± 1 nmol·mg protein^{-1} ($p < 0.05$) (Fig. 4). The reduction was accompanied by lower intracellular GTP levels, which dropped from 3.1 ± 0.2 to 2.1 ± 0.1 nmol·mg protein^{-1} in control and hypertrophied cells, respectively ($p < 0.01$) (Fig. 4). Creatine kinase and adenylate kinase facilitate the delivery of high energy phosphoryls to cellular ATP/GTP utilization sites (34, 48). In hypertrophied cardiomyocytes, the activities of both enzymes decreased. Adenylate kinase activity dropped from 565 ± 23 to 242 ± 7 nmol·min^{-1}·mg protein^{-1} ($n = 6, p < 0.001$) (Fig. 4). Creatine kinase activity was also reduced, dropping from 191 ± 16 to 66 ± 4 nmol·min^{-1}·mg protein^{-1} ($n = 6, p < 0.001$) (Fig. 4). Thus, hypertrophied cells have altered nucleotide levels and reduced the activities of the enzymes responsible for the delivery of nucleotides to nuclear pores.

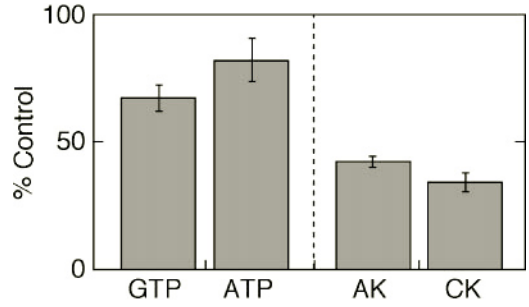

FIG. 4. **Change in nucleotide levels, creatine kinase, and adenylate kinase activities in hypertrophy.** In control and hypertrophied cardiomyocytes, ATP and GTP were measured using fluorometry and HPLC, whereas the activities of adenylate kinase (*AK*) and creatine kinase (*CK*) were measured by coupled enzyme assays. Values obtained in hypertrophy are expressed as the percent of control. Hypertrophy was induced by phenylephrine (100 μM, 48 h). Data were collected from 8 to 10 coverslips containing 500,000 to 1,000,000 cardiomyocytes obtained from separate cell isolations.

Closure of Nuclear Pores in Hypertrophy—Changes in cellular energetics can induce structural changes in cardiac nuclear pores (29). Thin electron microscopy sections of cardiomyocytes showed that nuclear pores were present at a similar density in control and hypertrophied cells with no detectable size difference (Fig. 5*a*). At this resolution, the diameter of the opening of nuclear pores was 51.0 ± 1.5 nm ($n = 30$) and 50.8 ± 1.2 nm ($n = 62$) for control and hypertrophied cells, respectively. Following the peeling of the sarcolemma to expose the nucleus (Fig. 5*b*), the nuclear envelope was scanned by atomic force microscopy. High resolution imaging of the cytoplasmic surface of individual nuclear pore complexes showed the characteristic toroid shape structure comprising a deep central pore surrounded by a ring-like distribution of peaks (Fig. 5*c*, *left*). In hypertrophy, the central pore appeared plugged (Fig. 5*c*, *right*). In fact, in control cells the majority of nuclear pore complexes displayed an open configuration of the central pore (66% of 131 nuclear pore complexes analyzed). In hypertrophied cells, however, a significantly lower percentage of nuclear pore complexes were open (36% of 182 nuclear pore complexes analyzed). Thus, although the overall structure of nuclear pore complexes is maintained, in hypertrophy the percentage of open pores available for nuclear import are reduced.

DISCUSSION

Processes involving cellular restructuring, such as hypertrophy, require *de novo* protein synthesis that depends upon the export of genetic material from the nucleus. It is yet unknown how cells support increased demands for nucleocytoplasmic communication because nuclear export and import compete for the same transport pathway through the nuclear pore. The present study establishes that hypertrophied cardiac cells direct traffic across the nuclear envelope through an adaptive

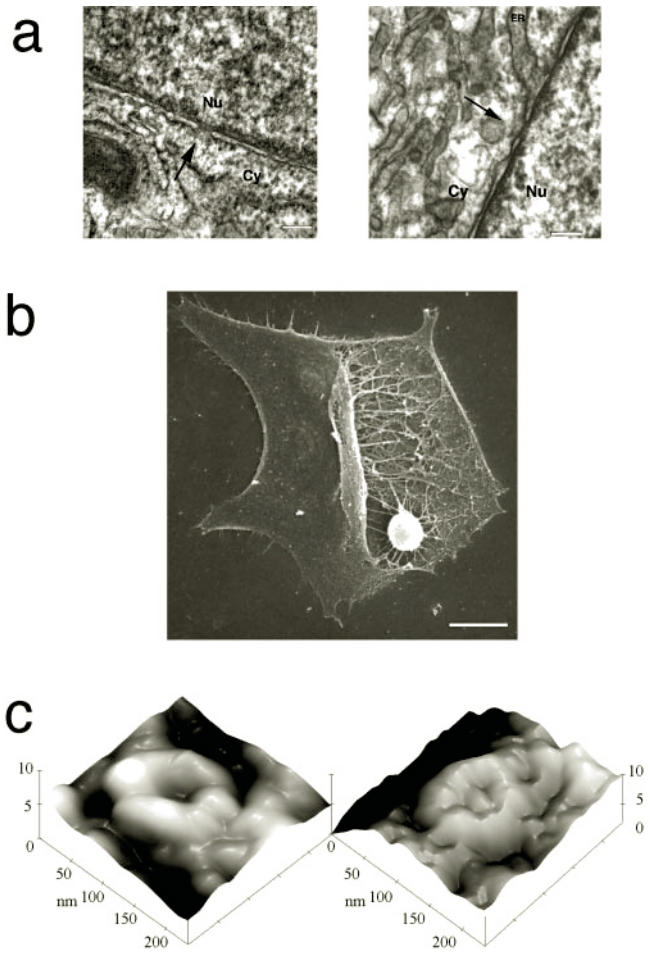

FIG. 5. **Plugging of nuclear pores in hypertrophy.** *a*, transmitted electron micrographs of the nuclear envelope separating the cytosol (*Cy*) from the nucleus (*Nu*) in control (*left*) and hypertrophied (*right*) cardiomyocytes. *Arrows* indicate individual nuclear pores with no significant difference in diameter observed in both conditions. *Horizontal bars*, 100 nm. In the *micrograph*, on the *right*, note the continuity of the nuclear cisterna with the lumen of the sarcoplasmic reticulum (*ER*). *b*, field-emission scanning electron microscopy of a sarcolemma-stripped cardiomyocyte. The nucleus, supported by the cytoskeletal scaffold, is exposed for further imaging by atomic force microscopy. *Horizontal bar*, 10 μm. *c*, atomic force microscopy of individual nuclear pore complexes from a control (*left*) and hypertrophied (*right*) cardiomyocyte. The open pore is characteristic of the majority of nuclear pore complexes in control, whereas a closed pore is characteristic of the majority of nuclear pore complexes in hypertrophy.

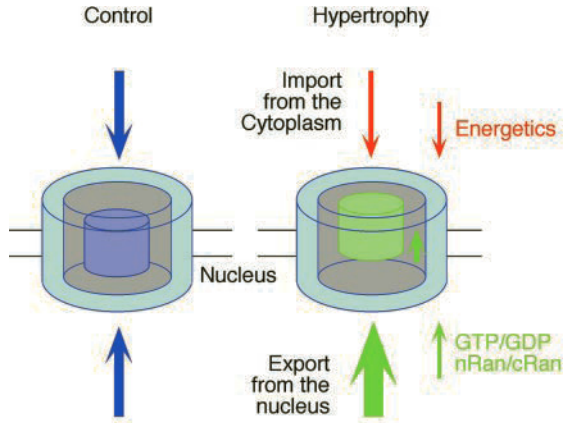

FIG. 6. **Transport regulation in hypertrophy.** Under control conditions (*left*), nuclear export and import share the same transport pathway through the nuclear pore. Under hypertrophy (*right*), enhanced export is favored over import because of the structural restriction (*i.e.* plugging of the cytosolic surface of the nuclear pore), impaired energy delivery to the pore (*i.e.* reduced phosphotransfer catalytic activity and nucleotide levels), and redistribution of nuclear transport factors (*i.e.* GTP/GDP ratio and Ran).

restriction of nuclear import. This is accomplished by remodeling nuclear pores and cellular energetics along with a redistribution of nuclear transport factors favoring nuclear export over import. Thus, this study uncovers a homeostatic mechanism by which cardiac cells suppress normal nuclear import activity to permit the gene export required in the development of cellular hypertrophy (Fig. 6).

The mechanism was demonstrated using two distinct hypertrophic stimuli, phenylephrine and angiotensin II, which produce myocardial hypertrophy through the activation of different receptors (12, 49). Previously, the inhibition of nuclear import was observed in cardiomyocytes depleted of cellular Ca^{2+} (29). Although in hypertrophy, the genes coding Ca^{2+} regulatory proteins can be down-regulated (1–3, 9, 13), it is unlikely that the down-regulation of nuclear import was attributable to disrupted Ca^{2+} homeostasis. Intracellular Ca^{2+} did not differ between control and agonist-treated cells (49), and the purinergic agonist ATP, which shares with phenylephrine and angiotensin II the ability to activate Ca^{2+}-mobilizing phosphoinositides without producing hypertrophy (12, 40, 42), however, did not decrease transport. Moreover, removal of the hypertrophy-inducing agent restored import, indicating the reversibility of the process. Thus, down-regulated nuclear transport appears associated with the hypertrophic process itself.

The crowding of the cytosol with an excess of newly synthesized actin filaments did not explain down-regulated nuclear transport in hypertrophied cells because the disruption of the actin cytoskeleton did not rescue nuclear import. Rather than a nonselective down-regulation of global nuclear transport, the hypertrophic signal primarily controlled the dynamics of active nuclear import. Indeed, hypertrophy was associated with the immediate loss of nuclear import of the 21-kDa histone H1, a chromatin protein imported into nuclei by active transport (37, 38), with no effect (or only late effects) on the passive diffusion of smaller molecules. In fact, even with advanced hypertrophy (24 h) no disruption in the nuclear translocation of dextrans was observed, suggesting that alterations in passive diffusion, in contrast to reduced active import, are not critical in the generation of the hypertrophic phenotype. Rather, a late reduction in the passive transport of 10-kDa dextrans (48 h) may be an epiphenomenon of advanced hypertrophy contributing to the maintenance of the phenotype.

What differentiates active import from passive diffusion is the requirement for a number of transport factors (14–18). Although ATP may serve as an energy source, GTP and GDP act as co-factors supporting the activity of guanine nucleotide-binding proteins, such as Ran, necessary for active nuclear transport (21, 32, 47, 50). The asymmetry in the Ran-GTP/Ran-GDP distribution determines the direction of nucleocytoplasmic transport. Ran-GDP on the cytoplasmic side of the nuclear envelope plus a source of ATP/GTP appears necessary for import, whereas Ran-GTP inside the nucleus is essential for nuclear export (47). In fact, the direction of transport through the nuclear pore can be inverted by high concentrations of cytoplasmic Ran-GTP (51). Thus, the observed increase in the GTP/GDP ratio, along with a redistribution of Ran into the nucleus, would favor nuclear export over import in hypertrophied cardiomyocytes.

In cells depleted of energy, molecules that are actively transported accumulate on the cytosolic surface of the nuclear membrane (29), indicating that targeting and docking to the nuclear pore may be energy-independent, whereas actual translocation requires an energy source (52). Nuclear transport is consis-

tently observed in the presence of ATP/GTP-regenerating systems (53) such as creatine kinase, which can support energy-dependent processes even at low nucleotide levels. In accordance with a disruption in the myocardial metabolism of purine and pyrimidine nucleotides reported in ventricular hypertrophy (54), we find that high energy-containing nucleotides and the activities of key phosphotransfer enzymes (33, 34, 55, 56) are reduced in hypertrophied cells. A compromised delivery of energy-rich phosphoryls, in conjunction with altered nucleotide levels, would also contribute to down-regulated nuclear import.

A decrease in the percentage of open nuclear pores on the cytosolic side may further limit available gateways for nuclear import in hypertrophy. The closing of the cytosolic mouth of nuclear pores has been associated with impaired import in cardiomyocytes (29). It has been suggested that nuclear export shares with nuclear import the same routes, namely the central channel of nuclear pore complexes (17). The net direction of transport would depend on the relative rates of export and import (17, 21). Evidence for the asymmetric closure of the nuclear and cytoplasmic faces of nuclear pores has been recently demonstrated (24). Therefore, the closing of the cytosolic side of nuclear pores, although leaving the nuclear side of the pore open, would favor nuclear export over import (Fig. 6).

Leptomycin B inhibits nuclear export upstream of the translocation through the nuclear pore complex by binding to the nuclear export mediator exportin and preventing the binding of other proteins for export (44–46, 57). The inhibition of nuclear export in hypertrophied cardiac cells using leptomycin B restored nuclear import. Thus, reversible down-regulated nuclear import may be a required adaptation as a necessity for increased nuclear export in hypertrophy. By down-regulating nuclear import, a hypertrophied cell would free routes for unobstructed export, securing the massive and fast exit of mRNA out of the nucleus to ribosomes for *de novo* protein synthesis.

Hypertrophied cells undergo profound phenotypic changes requiring the increased processing and delivery of genetic information across the nuclear membrane. This study provides the first evidence that hypertrophied cardiac cells support the demand for increased nucleocytoplasmic communication through an adaptive down-regulation of nuclear import compensating for the limited total nuclear transport capacity. The closure of the nuclear pore complex restricted import at the translocation step, whereas altered bioenergetics and nuclear factor redistribution favored export over import. Such cellular remodeling could guide traffic of genetic materials and other macromolecules across the nuclear envelope and thereby directly contribute to the development of the hypertrophic cellular phenotype.

Acknowledgments—We thank Drs. M. Hieda and Y. Yoneda (Osaka University) for the Ran antibody, Novartis and Dr. B. Wolff for the gift of leptomycin B, and Dr. P. Travo (European Advanced Imaging Center, CRBM, Montpellier) for assistance with three-dimensional deconvolution.

REFERENCES

1. Hunter, J. J., and Chien, K. R. (1999) *N. Engl. J. Med.* **341,** 1276–1283
2. McKinsey, T. A., and Olson, E. N. (1999) *Curr. Opin. Gen. Dev.* **9,** 267–274
3. Swynghedauw, B. (1999) *Physiol. Rev.* **79,** 215–262
4. Izumo, S., Lompre, A. M., Matsuoka, R., Koren, G., Schwartz, K., Nadal-Ginard, B., and Mahdavi, V. (1987) *J. Clin. Invest.* **79,** 970–977
5. Akhter, S. A., Luttrell, L. M., Rockman, H. A., Iaccarino, G., Lefkowitz, R. J., and Koch, W. J. (1998) *Science* **280,** 574–577
6. Depre, C., Shipley, G. L., Chen, W., Han, Q., Doenst, T., Moore, M. L., Stepkowski, S., Davies, P. J., and Taegtmeyer, H. (1998) *Nat. Med.* **4,** 1269–1275
7. Sussman, M. A., Lim, H., Gude, N., Taigen, T., Olson, E. N., Robbins, J., Colbert, M., Gualberto, A., Wieczorek, D., and Molkentin, J. D. (1998) *Science* **281,** 1690–1693
8. Thierfelder, L., Watkins, H., MacRae, C., Lamas, R., McKenna, W., Vosberg, H. P., Seidman, J. G., and Seidman, C. E. (1994) *Cell* **77,** 701–712
9. Chien, K. R., Knowlton, K. U., and Chien, S. (1991) *FASEB J.* **5,** 3037–3046
10. Pennisi, E. (1998) *Science* **279,** 1129–1131
11. Bishopric, N. H., Simpson, P. C., and Ordahl, C. (1987) *J. Clin. Invest.* **80,** 1194–1199
12. Sadoshima, J., and Izumo, S. (1997) *Annu. Rev. Physiol.* **59,** 551–571
13. Chien, K. R. (1999) *Cell* **98,** 555–558
14. Dingwall, C., and Laskey, R. (1992) *Science* **258,** 942–947
15. Nigg, E. A. (1997) *Nature* **386,** 779–787
16. Görlich, D., and Mattaj, I. W. (1996) *Science* **271,** 1513–1518
17. Ohno, M., Fornerod, M., and Mattaj, I. W. (1998) *Cell* **92,** 327–336
18. Pemberton, L., Blobel, G., and Rosenblum, J. (1998) *Curr. Opin. Cell Biol.* **10,** 392–399
19. Pante, N., and Aebi, U. (1996) *Science* **273,** 1729–1732
20. Corbett, A. H., and Silver, P. A. (1997) *Microbiol. Mol. Biol. Rev.* **61,** 193–211
21. Mattaj, I. W., and Englmeier, L. (1998) *Annu. Rev. Biochem.* **67,** 265–306
22. Cingolani, G., Petosa, C., Weis, K., and Muller, C. W. (1999) *Nature* **399,** 221–229
23. Chook, Y. M., and Blobel, G. (1999) *Nature* **399,** 230–237
24. Stoffler, D., Fahrenkrog, B., and Aebi, U. (1999) *Curr. Opin. Cell Biol.* **11,** 391–401
25. Yang, Q., Rout, M. P., and Akey, C. W. (1998) *Mol. Cell* **1,** 223–234
26. Perez-Terzic, C., Pyle, J., Jaconi, M., Stehno-Bittel, L., and Clapham, D. E. (1996) *Science* **273,** 1875–1877
27. Stehno-Bittel, L., Perez-Terzic, C., and Clapham, D. E. (1995) *Science* **270,** 1835–1838
28. Rakowska, A., Danker, T., Schneider, S., and Oberleithner, H. (1998) *J. Membr. Biol.* **163,** 129–136
29. Perez-Terzic, C., Gacy, A. M., Bortolon, R., Dzeja, P. P., Puceat, M., Jaconi, M., Prendergast, F. G., and Terzic, A. (1999) *Circ. Res.* **84,** 1292–1301
30. Moore, J. D. (2001) *Bioessays* **23,** 77–85
31. Jaconi, M., Bony, C., Richards, S., Terzic, A., Arnaudeau, S., Vassort, G., Puceat, M. (2000) *Mol. Biol. Cell* **11,** 1845–1858
32. Hieda, M., Tachibana, T., Yokoya, F., Kose, S., Imamoto, N., Yoneda, Y. (1999) *J. Cell Biol.* **144,** 645–655
33. Meyer, N., Jaconi, M., Landopoulou, A., Fort, P., and Puceat, M. (2000) *FEBS Lett.* **478,** 151–158
34. Dzeja, P. P., Vitkevicius, K. T., Redfield, M. M., Burnett, J. C., and Terzic, A. (1999) *Circ. Res.* **84,** 1137–1143
35. Dzeja, P. P., Pucar, D., Redfield, M. M., Burnett, J. C., and Terzic, A. (1999) *Mol. Cell. Biochem.* **201,** 33–40
36. Thomas, J. O. (1999) *Curr. Opin. Cell Biol.* **11,** 312–317
37. Breeuwer, M., and Goldfarb, D. S. (1990) *Cell* **60,** 999–1008
38. Jäkel, S. Albig, W., Kutay, U., Bischoff, F. R., Schwamborn, K., Doenecke, D., and Görlich, D. (1999) *EMBO J.* **18,** 2411–2423
39. Greber, U. F., and Gerace, L. (1995) *J. Cell Biol.* **128,** 5–14
40. Post, G. R., Goldstein, D., Thuerauf, D. J., Glembotski, C. C., and Brown, J. H. (1996) *J. Biol. Chem.* **271,** 8452–8457
41. Perez-Terzic, C., Jaconi, M., and Clapham, D. E. (1997) *Bioessays* **19,** 787–792
42. Puceat, M., and Vassort, G. (1996) *Biochem. J.* **318,** 723–728
43. Terzic, A., and Kurachi, Y. (1996) *J. Physiol. (Lond.)* **492,** 395–404
44. Kudo, N., Matsumori, N., Taoka, H., Fujiwara, D., Schreiner, E. P., Wolff, B., Yoshida, M., and Horinouchi, S. (1999) *Proc. Natl. Acad. Sci. U. S. A.* **96,** 9112–9117
45. Wolff, B., Sanglier, J. J., and Wang, Y. (1997) *Chem. Biol.* **4,** 139–147
46. Ossareh-Nazari, B., Bachelerie, F., and Dargemont, C. (1997) *Science* **278,** 141–144
47. Moore, M. S. (1998) *J. Biol. Chem.* **273,** 22857–22860
48. Dzeja, P. P., and Terzic, A. (1998) *FASEB J.* **12,** 523–529
49. Terzic, A., Puceat, M., Vassort, G., and Vogel, S. (1993) *Pharmacol. Rev.* **45,** 147–175
50. Brodsky, A. S., and Silver, P. A. (1999) *Nat. Cell Biol.* **1,** 66–67
51. Nachury, M. V., and Weis, K. (1999) *Proc. Natl. Acad. Sci. U. S. A.* **96,** 9622–9627
52. Michael, W. M., Choi, M., and Dreyfuss, G. (1995) *Cell* **83,** 415–422
53. Englmeier, L., Olivo, J. C., and Mattaj, I. W. (1999) *Curr. Biol.* **9,** 30–41
54. Swain, J. L., Sabina, R. L., Peyton, R. B., Jones, R. N., Wechsler, A. S., and Holmes, E. W. (1982) *Proc. Natl. Acad. Sci. U. S. A.* **79,** 655–659
55. Janssen, E., Dzeja, P. P., Oerlemans, F., Simonetti, A. W., Heerschap, A., Haan, A., Rush, P. S., Terjung, R. R., Wieringa, B., and Terzic, A. (2000) *EMBO J.* **19,** 6371–6381
56. Pucar, D., Janssen, E., Dzeja, P. P., Juranic, N., Macura, S., Wieringa, B., and Terzic, A. (2000) *J. Biol. Chem.* **275,** 41424–41429
57. Fukuda, M., Asano, S., Nakamura, T., Adachi, M., Yoshida, M., Yanagida, M., and Nishida, E. (1997) *Nature* **390,** 308–311